



## Assessing Geospatial Accuracy in Mapping Applications: A Focus on Google Earth

Thaar Alqahtani <sup>1\*</sup>

<sup>1</sup> Department of Civil Engineering, College of Engineering, Prince Sattam Bin Abdulaziz University, Alkharj 11942, Saudi Arabia.

Received 29 April 2024; Revised 30 June 2024; Accepted 09 July 2024; Published 01 August 2024

### Abstract

Google Earth, among other online mapping platforms, offers an interactive mapping platform that has become indispensable for academic and research applications. It serves as a primary reference and a foundational tool for map creation, providing open-source, cost-free imagery that meets the user needs of the mapping community. As a contemporary repository of high-resolution images of Earth's landmass, Google Earth has vast potential for scientific exploration and remains an underexploited resource. Its rapid expansion and consistent reliability make it a favored source for mapping and routing tasks. However, this research underscores the crucial aspect of Google Earth's positional accuracy, which is at the heart of this study. A comparative analysis between the positional accuracy of Google Earth and traditional ground surveying maps was conducted. The Wilcoxon rank test and quantitative methods were used to evaluate coordinate discrepancies, revealing significant discrepancies between the two datasets. This study aims to provide a rigorous assessment of Google Earth's utility and accuracy in scientific and academic contexts, emphasizing its role and reliability as a critical resource for researchers and practitioners in the field of mapping. The results revealed displacement changes in both the northing and the easting coordinates. For the northing coordinates, the displacement increases when moving eastward and decreases when moving westward. For the easting coordinates, the displacement increases when moving northward and decreases when moving southward. This pattern highlights spatial discrepancies and the varying impact of location on the dataset's accuracy, emphasizing the need for targeted corrections to enhance data accuracy. These key findings provide valuable insights that could significantly contribute to optimizing mapping practices and efficiently exploiting this vast, yet underexplored, digital resource.

*Keywords:* Google Earth; Mapping; Geospatial Accuracy; Vector Length Error; Change in Coordinates.

### 1. Introduction

Advances in remote sensing technologies and applications have significantly enhanced the temporal and spatial resolution of captured data across a broader range of spectral signatures, fundamentally transforming our methods of Earth observation [1]. The swift progress in information and communication technologies offers an unparalleled wealth of information, enabling a more detailed and comprehensive understanding of our planet's state than traditional methods could provide [2]. In a transformative approach to the digital representation of our planet, Google Earth (GE) plays a key role in humanity's efforts to comprehend our surroundings and manage resources more effectively. It stands out for its contributions toward realizing the goals set in the United Nations 2030 Agenda for Sustainable Growth [3]. Remarkably, the widespread popularity of GEs stems from their superior visualization capabilities, straightforward accessibility to an extensive array of geospatial information, and ability to integrate a universal coordinate framework,

\* Corresponding author: [t.alqahtani@psau.edu.sa](mailto:t.alqahtani@psau.edu.sa)

<http://dx.doi.org/10.28991/CEJ-2024-010-08-012>



© 2024 by the authors. Licensee C.E.J, Tehran, Iran. This article is an open access article distributed under the terms and conditions of the Creative Commons Attribution (CC-BY) license (<http://creativecommons.org/licenses/by/4.0/>).

despite scalability limitations [4]. As a digital globe, GEs facilitate seamless connections across global locales, providing open access to geospatial data and thereby fostering international collaboration aimed at achieving sustainable development goals (SDGs) [5]. There is an ongoing commitment among global policymakers to pursue sustainable development initiatives aligned with the SDGs [4]. These goals are fundamentally linked to geospatial data, underscoring its importance; for instance, the concept of location-based services would hardly be feasible in the absence of such data [6].

The role of GEs extends beyond data sharing, bridging the digital divide between the Global North and South by democratizing access to vital geospatial data for cross-border partnerships and cooperative efforts [7, 8]. Recently, GE has become a pivotal resource in diverse research areas, including social sciences [9], atmospheric studies [10], urban research [11], and disaster management [12], indicating its significance in global environmental change research. Moreover, GE has found extensive application in educational contexts, particularly in geography instruction, thanks to its unparalleled capability for rendering virtual representations of the Earth [13]. The benefits of utilizing GE span six distinct domains: visualization and data exploration, data gathering, validation, data merging and compatibility, simulation, and user-friendliness [14]. While the popularity of GE as a digital platform continues to grow, owing to its user-friendly visual features, it is not without its drawbacks. These limitations include varying quality of imagery, restricted options for quantitative analysis, an absence of tools for in-depth analytical work, and limitations in conducting accurate worldwide spatial simulations [4, 15].

The visualization capabilities of GEs have significantly contributed to various domains, including internet GIS [16], land conversion studies [17], urban household surveys [18], health geography research [19], real estate [20], lake mapping [21], relief efforts [22], and land use mapping [19]. The historical imagery feature of the GE, which offers snapshots from different times, proves invaluable for studies focused on changes in land use [19]. Its accessible and user-friendly interface offers a convenient platform for interactive data analysis and algorithm development [23]. Moreover, users can integrate and manage their own data and collections while utilizing Google's cloud resources for processing [24, 25]. The application of GE in scholarly endeavors spans several critical areas: visualization, data collection and verification, the integration of data, the publication of research findings, modeling, exploratory data analysis, and aiding in decision-making processes [4].

The advent of spatial technologies integrated with the internet has birthed virtual globes, enhancing global access to geospatial data [26]. These platforms offer interactive experiences, allowing users to navigate the globe through various perspectives, angles, and data overlays, whether they are representations of real or conceptual geographical information [27]. Despite GE's widespread use and trust in its precision, there is an implicit assumption among its user base regarding its accuracy and reliability [28]. Accurate and up-to-date land cover information is essential for land managers and policymakers in developing and implementing effective conservation strategies and policies [29]. However, creating high spatial resolution land cover maps over large areas poses significant challenges. These challenges include managing large volumes of data, developing complex training and validation datasets, addressing data availability issues, and addressing heterogeneous data and landscape conditions [2, 30, 31]. Some specialized software programs address these challenges by integrating expert knowledge into the analytical workflow for land cover mapping [1, 32].

Concerns have been raised about the dependability of GE images due to the obscure nature of their metadata, which includes information about the sensors used, the resolution of the imagery, and the methods employed for overlaying and stitching together images [33]. It has been noted that Google's geographic data products should be considered approximations, as their accuracies are not officially validated [34]. Google has demonstrated reluctance in disclosing detailed accuracy specifications of the GE database [35]. Furthermore, GE images are not orthorectified, meaning that they lack the adjustments necessary for a flat map representation and do not meet photogrammetric precision standards [36]. The vagueness of the horizontal precision of the imagery might lead to the misrepresentation of features and subsequent analytical errors [33], casting doubts on the suitability of GE imagery for tasks requiring exactitude, such as precision engineering assessments and autonomous navigation systems [37]. The tradition of presenting coordinates with a level of precision that surpasses their actual accuracy might falsely assure users of the information's reliability [38]. Furthermore, Google officials have conceded that the coordinates and data featured in their geographic products are merely estimative, with no guarantees concerning their precision [39]. An examination of historical GE images revealed that the degree of horizontal displacement can fluctuate over time [40].

In recent years, the integration of GEs has significantly advanced geospatial studies, particularly in assessing geospatial accuracy. For instance, Bajaj et al. [41] used GE to monitor changes in mangrove forest cover and carbon stocks in the lower Mekong region, achieving 92.10% accuracy. Zurqani [42] estimated forest canopy cover in Arkansas

with accuracies between 83.31% and 94.35% using high-resolution imagery and machine learning within GE. Ganjirad & Bagheri [43] mapped land use and land cover using Landsat 8 for weather models and achieved 94.92% accuracy. Habibie et al. [44] applied GE with deep learning to forecast land utilization in Jambi district, achieving 79.59% accuracy. Merchant et al. [45] mapped Arctic wetlands, achieving over 89% accuracy, demonstrating the effectiveness of GE with large datasets [46]. Prasai et al. [2] used the GEE Python API for LULC classification in Florida and achieved 86% accuracy, highlighting the cost-effectiveness of GE. These studies collectively underscore the versatility and robustness of GEs in remote sensing and environmental monitoring. However, GE offers the capability to display a variety of imagery types superimposed upon the Earth's surface and functions as a client for web map services [47]. The foundational technology of GE traces its origins back to intrinsic graphics during the late 1990s. The project to provide 3D representations of urban areas commenced in 2012 [48].

By the beginning of 2016, this coverage had grown from just 21 cities across four nations to several hundred cities spanning more than 40 countries, covering all U.S. states and every continent except for Antarctica [7]. GE's very high-resolution satellite imagery boasts a spatial resolution of less than 5 meters [49]. However, the clarity of these images varies according to the satellite's specifics, such as its altitude and the equipment it carries [50]. Contrary to appearing seamless and uniform, GE imagery is actually a compilation of various images taken at different times, showcasing spatial resolutions that range from 15 meters to as much as 10 centimeters, and is sourced from various providers [49]. Due to the diverse origins of these images, there is variability in their positional accuracy and spatial resolution [50]. Where necessary, satellite imagery is augmented with aerial photos, which offer greater detail. In areas lacking high-resolution images, GE switches to Landsat imagery as a standard fallback [51].

The concern regarding the accuracy of GE positioning has been somewhat overlooked by the global research community. There appears to be a noticeable gap in efforts to evaluate the geospatial precision of mapping, especially within the context of Saudi Arabia. Furthermore, an exploration of the literature did not reveal any investigations addressing the precision of historical imagery in GE. Positional accuracy is typically categorized into different dimensions [52]. There are some instances of geo-registration errors and significant horizontal discrepancies within GE imagery [34]. However, the increasing reliance on online mapping applications, particularly GEs, by the academic community underscores the pivotal role these platforms play in facilitating a broad spectrum of mapping and scientific endeavors. GE's expansive repository of Earth's geographical data offers unprecedented opportunities for scientific exploration, yet its rapid expansion and the voluminous nature of its datasets have led to underutilization of its full potential. This study critically assesses the geospatial accuracy of GE, addressing a key concern for users who rely on its data for precise mapping and routing.

This research aimed to validate the reliability and accuracy of GE, which is essential for its use in academic and professional projects. By examining the positional accuracy of GEs, this study underscores its importance in academia and aims to enhance its applicability and reliability for future geospatial research. The literature highlights the extensive application of GE in various fields and its role in facilitating global collaborations through geospatial data. However, despite its popularity and utility, there is a significant gap in comprehensive evaluations of the positional accuracy of GEs, particularly compared to traditional ground surveying maps. This gap is further pronounced in specific regional contexts, such as Saudi Arabia, and in the accuracy of historical imagery provided by GE. Current studies have not sufficiently addressed the discrepancies and geo-registration errors that may impact the precision and reliability of GE for high-accuracy tasks.

The proposed approach to fill this gap involves conducting a detailed comparative analysis between GE coordinates and those obtained from traditional ground surveying methods using the Wilcoxon rank statistical test and other quantitative methods. By assessing the coordinate discrepancies and spatial variations, this study aims to provide a rigorous evaluation of GE's geospatial accuracy, thereby enhancing its reliability and applicability for academic and professional use. For the first time, this study represents an investigation into assessing geospatial accuracy in mapping applications, specifically focusing on Google Earth, conducted in Saudi Arabia. Furthermore, it uniquely integrates both quantitative and qualitative analyses, employing methods such as the Wilcoxon signed-rank test, which have been largely absent in previous research. This approach will not only validate GE's accuracy but also offer targeted corrections to improve data precision, ultimately optimizing mapping practices and fully exploiting the potential of this underutilized digital resource. In brief, the findings of this study provide valuable insights into the positioning accuracy of Google Maps within the context of Saudi Arabia, contributing significantly to the current research community. Figure 1 shows the structural diagram of the article.

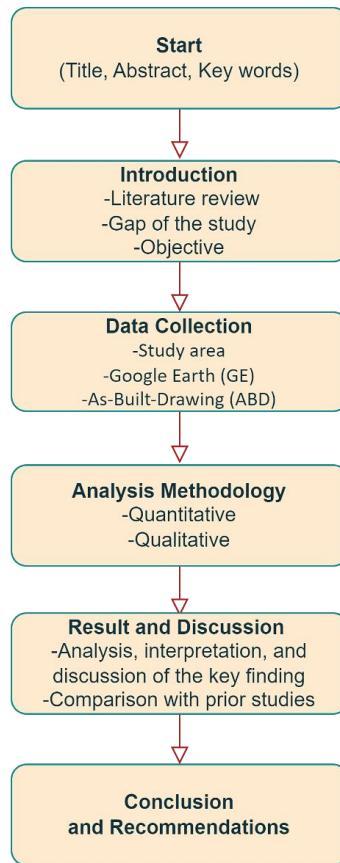


Figure 1. Structural Diagram of the Article

## 2. Research Methodology

### 2.1. Study Area

The study area was at Al-Kharj Province, Saudi Arabia, at Prince Sattam Bin Abdulaziz University (PSAU). Al-Kharj is located in the central region of Saudi Arabia, southeast of the capital, Riyadh, approximately 77 kilometers (approximately 48 miles) away. Figure 2 depicts a map of Al-Kharj city and the study area. Al-Kharj falls within the Universal Transverse Mercator (UTM) Zone 38 under the World Geodetic System 1984 (WGS 1984) ellipsoid. The campus is geographically located between longitudes 47° 16' 00" E – 47° 17' 00" E and latitudes 24° 08' 30" N – 24° 09' 30" N. The campus area is approximately 960,000 sq meters at a level terrain. Thirty-six buildings were selected from various locations across the campus, featuring a variety of shapes, such as squares, rectangles, triangles, and pentagons, as shown in Figure 3. These location spots were divided into four zones, namely, Zone 1, Zone 2, Zone 3, and Zone 4, which represent the southern, mid-southern, mid-northern, and northern campus locations, respectively.

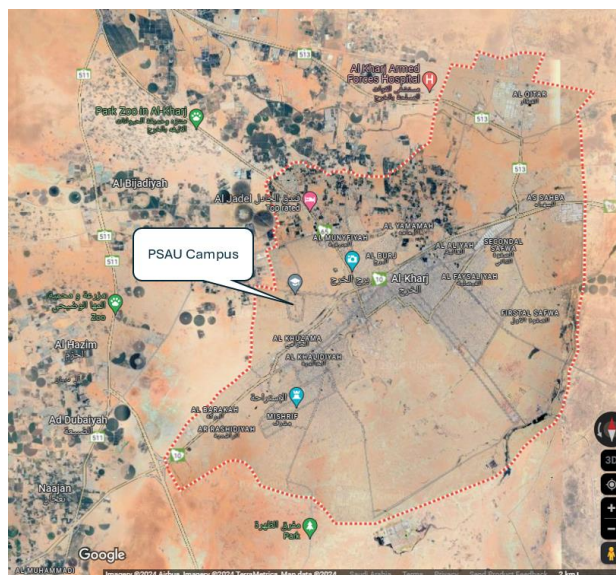


Figure 2. Map of the city of AL-Kharj and study area, Saudi Arabia



Figure 3. Aerial photography of the study area

**2.2. Data Collection**

The datasets were collected by extracting a total of 144 geospatial points from GE. These points were accurately positioned and meticulously selected across the study area. In parallel, a comparable set of points was derived from as-built drawing (ABD) that meticulously documented the horizontal coordinates (east and north) of these locations. The source of the ABD was the Operation and Maintenance Department at PSAU, ensuring the reliability and institutional oversight of spatial data for the analysis conducted in this study. However, this study aimed to delineate a systematic approach to evaluating the discrepancies in station coordinates (east, E; north, N) obtained from two distinct data sources: GE and ABD. The extracted data were initially obtained from station coordinates (E, N) from both sources. The primary objective was to calculate the differences between the coordinates from these sources, thereby quantifying any discrepancies in spatial data representation via Wilcoxon tests. Then, the differences between these station coordinates were used to calculate the vector length errors (VLEs). Furthermore, the length of polygons' sides, representing segments of interest within the study area, were calculated using data from both sources. These calculated lengths were then subjected to a comparative analysis, aiming to quantify the variability and consistency across the two datasets. Besides, descriptive statistics were deployed to determine the differences between the East (E) and North (N) coordinates. This step involved summarizing the data through measures of central tendency, dispersion, and distribution shape, thereby providing a comprehensive overview of the spatial discrepancies encountered. Figure 4 depicts the methodology flowchart.

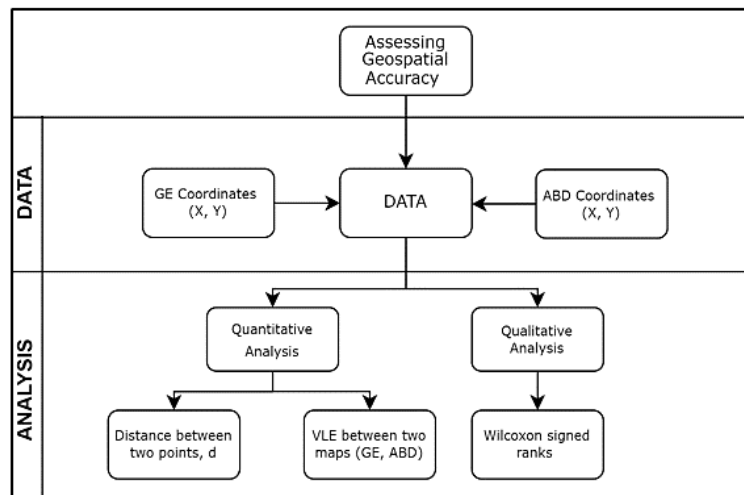


Figure 4. Methodology flowchart

## 2.3. Analytical Methods

### 2.3.1. Wilcoxon Signed-Rank Test

The Wilcoxon signed ranks test is a nonparametric test procedure for analyzing matched-pair data based on differences. The signed ranks test is more conservative than the more familiar t-test [53]. Moreover, the application of the Wilcoxon signed-rank test across various data types and its robustness under nonnormal conditions make it a preferred choice in many geospatial studies. For example, Elwood et al. [54] utilized the Wilcoxon signed-rank test to compare GIS-based measurements with traditional surveying methods and reported similar patterns of significant coordinate differences but consistent distance measurements. This consistency across different studies underscores the reliability of the Wilcoxon signed-rank test in handling geospatial data, particularly when normality assumptions are violated. The Wilcoxon signed ranks test was used to examine the relationship between each coordinate pair (i.e.,  $\Delta E$  and  $\Delta N$ ). The tested hypotheses are as follows:

**Null hypothesis:** There are no significant differences between the coordinates obtained from the GE and the coordinates obtained from the ABD.

**Alternative hypothesis:** There are significant differences between the coordinates obtained from the GE and the coordinates obtained from the ABD.

The test procedure is as follows: For this study, the sample size (i.e.,  $N$ ) is 144, and there are a total of  $2N$  data points  $x_{1,i}$  and  $x_{2,i}$ ,  $i \rightarrow$  the pair number.

- For each  $i$ ,  $|x_{1,i} - x_{2,i}|$  and the sign of the difference are calculated.
- The pairs with  $|x_{1,i} - x_{2,i}| = 0$  are excluded, and the remaining pairs  $N_r$  are ordered in ascending order.
- Ranked Paris  $R_i$  is calculated by ranking the pairs starting with the pair with the smallest nonzero absolute difference as 1. The ties received a rank equal to the average of the ranks they span.
- The sum of the ranks for positive and negative differences is computed. The smallest value is used for the test statistic ( $W$ ), which is compared with the critical value ( $W_{\text{critical}}$ ) from the Wilcoxon Table.

### 2.3.2. Quantitative Analysis

The differences in coordinates between reference points on the ABD and their corresponding points on the GE were employed as a primary metric. This involved subtracting the coordinates of points on the ABD from those of the corresponding coordinate points in the GE. The differences in eastings and northings are given as follows:

$$\Delta E = E_{ABD} - E_{GE} \quad (1)$$

$$\Delta N = N_{ABD} - N_{GE} \quad (2)$$

where  $\Delta E$  is Differences in Eastings,  $E_{ABD}$  is East selected points on the ABD,  $E_{GE}$  is North selected points on the GE,  $\Delta N$  is Differences in Northings,  $N_{ABD}$  is East selected points on the ABD,  $N_{GE}$  is North selected points on the GE.

The VLE is defined as the distance between two pairs of coordinates from two different datasets (GE and ABD) (Figure 5) and can be calculated via the following formula:

$$VLE = \sqrt{\Delta E^2 + \Delta N^2} \quad (3)$$

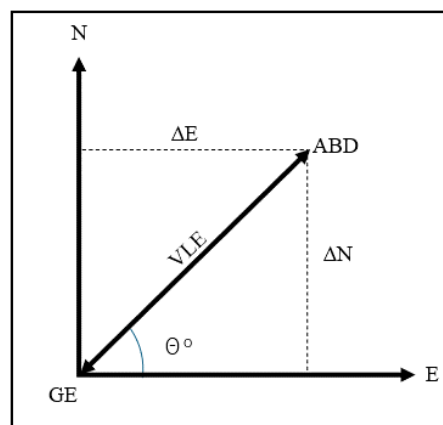


Figure 5. Illustration of the vertical length error/shift between a point on the reference ABD and the corresponding position on the GE

This methodological framework underpins this study's analytical rigor, ensuring a thorough and systematic examination of spatial data discrepancies between GEs and ABDs. This approach aims to offer insights into the precision and reliability of spatial data derived from different sources, contributing valuable knowledge to the field of geospatial analysis.

### 3. Results and Discussion

#### 3.1. Statistical Tests

In the analysis of the datasets comprising paired observations from 144 geospatial points, the Wilcoxon signed-rank test [55] was selected as the statistical analysis tool because this test has the ability to effectively handle paired samples without presupposing a normal distribution of the data differences [53]. A preliminary examination of the dataset suggested deviations from normality, thereby underscoring the appropriateness of a nonparametric approach. The Wilcoxon signed-rank test, known for its applicability across various data types and its robustness in situations where the normality assumption is violated, offers an optimal methodological fit [53]. The Wilcoxon signed-rank test was conducted to compare GE coordinates and ABD coordinates. For the eastern points,  $W=0.0$  and a p-value of  $2.23 \times 10^{-25}$  indicate a statistically significant difference between the paired variables. For the North points, the test statistic was  $W=359.0$ , and the p-value was approximately  $3.19 \times 10^{-22}$ . This extremely low p-value indicates a statistically significant difference between the paired observations of the North points. The Wilcoxon signed-rank test was then applied to the length of the polygon side from GE, and ABD yielded a test statistic of  $W=4625.0$  and a p-value of approximately 0.235. This p-value was greater than the typical significance level of 0.05, indicating that there was no significant difference in the median values of the estimated distances between the GE- and ABD-measured distances.

The paradigm of geospatial data collection is evolving from being data-sparse to data-rich. In the past, capturing geospatial data required technically demanding, highly accurate, expensive, and complex devices, often making the measurement process an art in itself. However, the current scenario shows a significant shift, where geospatial data acquisition has become a commonplace activity integrated into everyday devices such as smartphones, which are widely used [56, 57]. These modern devices can capture environmental geospatial information with remarkable geometric accuracy, temporal resolution, and thematic detail. Additionally, they are compact, user friendly, and capable of collecting data, sometimes even without conscious effort [58]. Similarly, Goodchild & Li [59] highlighted notable discrepancies in geospatial data arising from variations in data collection methods, sensor accuracies, and processing techniques. Li et al. [60] supported these observations, indicating that different data sources could lead to considerable differences in spatial data accuracy. Moreover, the impact of these discrepancies on spatial analysis necessitates a thorough examination of data source characteristics to ensure accuracy. This notion is further corroborated by recent research, including a study by West Meiers et al. [61], which noted significant differences in urban density over time when using satellite imagery for geospatial impact assessments. Advances in geospatial artificial intelligence (GeoAI), as discussed by Li & Hsu [62], have also underscored the capacity of AI to detect subtle discrepancies in geospatial data, enhancing the precision of spatial analytics. Despite significant differences in the coordinate data, consistency in the distance measurements between points was maintained. This finding supports earlier research by Fisher and Tate [63], which suggested that discrepancies in positional data do not necessarily translate into differences in measured distances. This stability, as demonstrated in further studies [62, 64], is vital for applications requiring accurate distance estimations, such as in urban planning and infrastructure development, where GeoAI techniques can enhance data integration and maintain measurement consistency despite positional variances. It has also been reported that positional accuracy and referencing can vary widely [65]. This range includes highly precise coordinates, relative positions, and information that either lacks geometric reference altogether or is only implicitly identified through location names [56]. In this manner, it becomes feasible to utilize big data across a broad spectrum of practical applications. Achieving this would necessitate an enhanced database structure and, specifically, a highly adaptable spatial statistical analysis process.

#### 3.2. Changes in Coordinates

The change in Easting coordinates between the GE and ABD datasets across four campus zones provides several critical insights. Figure 6 illustrates the displacement changes in Easting coordinates between the GE and ABD datasets across four campus zones. In zone 1 (south), there are eight points with minimal displacement, ranging from a maximum of 23.66 meters to a minimum of 22.90 meters, with an average displacement of 23.32 meters. Zone 2 (mid-south) includes 109 points and shows a displacement range from a maximum of 36.45 meters to a minimum of 25.10 meters, averaging 29.15 meters. The displacement values in zones 3 (mid-north) and 4 (north) exhibit a pronounced upward trend, indicating significant and increasing discrepancies. Zone 3 has 14 points with displacements ranging from a maximum of 48.03 meters to a minimum of 45.31 meters, with a mean of 46.67 meters. Zone 4 has 13 points with displacements ranging from a maximum of 61.17 meters to a minimum of 57.93 meters, with a mean of 59.15 meters. This trend in the northern areas of the campus is likely due to distortion at the edge of UTM Zone 38 [66]. In summary, while the southern zones maintain minimal displacement, the mid-north and northern zones show greater and greater discrepancies in Easting coordinates. Similarly, these findings are consistent with previous research highlighting the challenges of positional accuracy in geospatial data, particularly at the edges of UTM zones. For instance, Li et al. [64] emphasized the increased positional errors in satellite imagery near the boundaries of UTM zones. This boundary effect

can exacerbate coordinate distortions, as seen in our analysis of the northern zones. Similarly, the growing accessibility of land-use information derived from satellite imagery has significantly enhanced researchers' ability to model land-use at the microlevel [67]. Numerous studies utilize early satellite data to model land-use, particularly in developing regions where alternative data sources are scarce. These models explore various land-use issues, including agricultural trends [68], climate change impacts [69], wildlife habitat loss [70], deforestation [71], and ecosystem services [72]. The advent of recent satellite-based land-use datasets, such as raster datasets, which offer high-resolution contiguous spatial coverage across extensive areas, prolonged temporal coverage, and specific land cover classifications (e.g., rye or winter wheat), is opening up new avenues for future research [73].

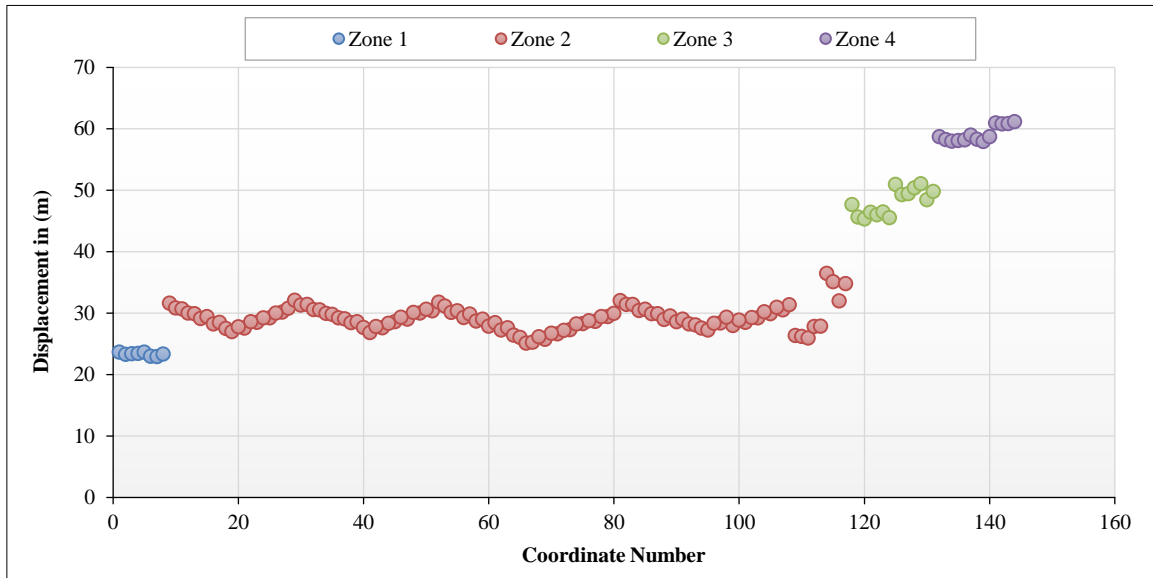


Figure 6. The displacement changes in Easting coordinates across four campus zones by location

The variation in Northing coordinates is influenced by the location of points on the PSAU campus, whether they are situated to the east or west. Figure 7 presents the distribution of data points on both sides of the campus. On the east side, Zone 1 includes 8 points, Zone 2 encompasses 100 points, and Zone 3 contains 7 points, totaling 115 points. In contrast, on the west side, Zone 2 has 9 points, Zone 3 has 7 points, and Zone 4 has 13 points, resulting in a total of 29 points. The data revealed that the displacement change in the Northing coordinates tends to increase when moving eastward, whereas it decreases when moving westward. This pattern highlights the spatial discrepancies and the varying impact of location on the dataset's accuracy. Similarly, research has identified significant spatial discrepancies among various cropland datasets, largely due to the high omission rates of croplands in Africa, particularly in Tanzania, Kenya, and Somalia [74]. A comparison of three datasets revealed substantial disagreement (43%) in mapping vegetation types such as forest, shrubland, grassland, and cropland in mountainous mining regions and the Sahel zone in Africa [75]. Despite these findings, there is limited research investigating the underlying causes of these discrepancies, particularly in the mapping of African croplands [76].

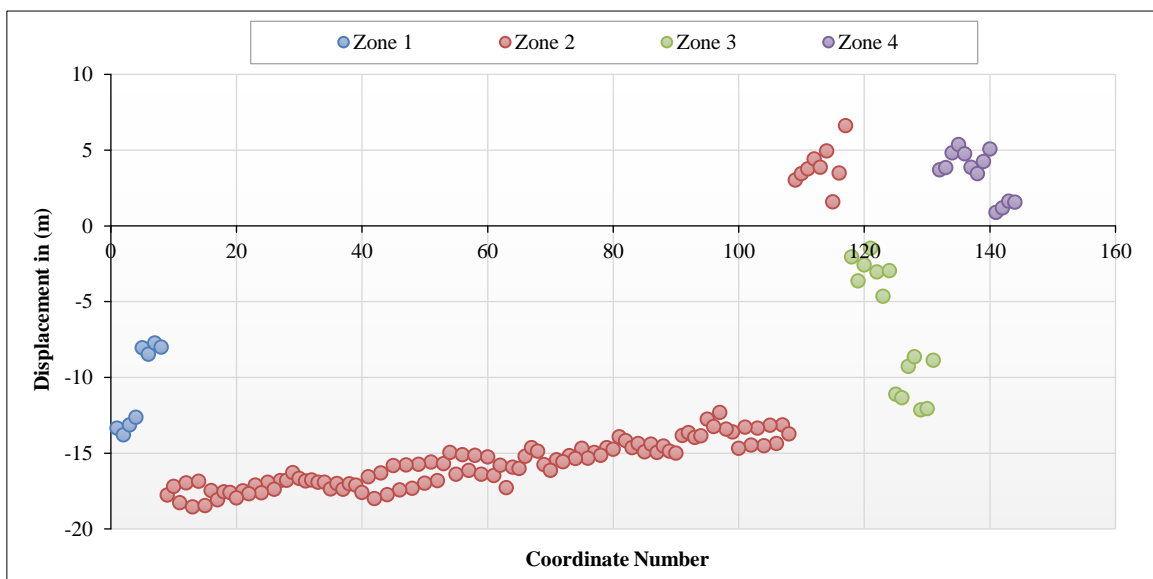


Figure 7. The displacement changes in Northing coordinates across four campus zones by location

In Zone 1 (east), there are eight points with displacements ranging from a maximum of -13.78 meters to a minimum of -7.72 meters, with an average displacement of -10.64 meters. Zone 2 (east) includes 100 points and shows a displacement range from a maximum of -12.30 meters to a minimum of -18.53 meters, averaging -15.79 meters. Zone 2 (west) includes 9 points and shows a displacement range from a maximum of 6.63 meters to a minimum of 1.59 meters, averaging 3.92 meters. Zone 3 (east) has 7 points with displacements ranging from a maximum of -8.62 meters to a minimum of -12.13 meters, with a mean displacement of -10.48 meters. Zone 3 (west) also has 7 points with displacements ranging from a maximum of -1.47 meters to a minimum of -4.64 meters, with a mean displacement of -2.90 meters. Zone 4 has 13 points with displacements ranging from a maximum of 13.99 meters to a minimum of 0.83 meters, with a mean displacement of 7.14 meters. Similarly, the observed skewness in a specific direction, which strongly suggests the presence of a systematic error, needs to be considered when utilizing imagery [7]. Nonetheless, GE continues to offer significant benefits due to its user-friendliness and contextual awareness, and additional research in other areas is necessary to ascertain whether this skewness is a widespread issue with GE imagery.

The analysis of displacement changes in Easting and Northing coordinates between the GE and ABD datasets across four zones revealed significant shifts in the coordinates. Figure 6 shows an example of coordinate shifting. The UTM coordinate system divides the globe into sixty north-south zones, each spanning 6 degrees of longitude. UTM Zone 38 [66] covers the area between longitudes 42°E and 48°E. The campus is located at the edge of this zone, specifically between 47° 16' 00" E and 47° 17' 00" E, which exacerbates coordinate distortions. These findings are consistent with previous studies that investigated the impact of geographical positioning on geospatial data accuracy. For instance, Elwood et al. [54] reported that areas near the edges of UTM zones or other coordinate system boundaries often suffer from higher positional inaccuracies. This phenomenon is primarily due to the inherent distortion effects of the map projection systems used in these zones. In addition, recent advancements in geospatial technologies and methodologies have highlighted the need for precise calibration and validation of geospatial data in complex environments.

Meiers et al. [61] emphasized that accurate geospatial analysis requires careful consideration of positional errors and targeted corrections, especially in regions prone to high distortion levels. It has been reported that numerous projects have focused on land cover dynamics, particularly in map comparisons for change detection analysis. Research indicates that even minor location errors can significantly impact the accuracy of change detection [77], necessitating precise registration to ensure that the error rate remains below 10% [78]. Moreover, the heterogeneity of land cover influences the effect of positional error; more fragmented land cover maps exacerbate change detection errors due to positional inaccuracies [79]. To mitigate the impact of positional errors on change detection accuracy, aggregation-based or object-based methods have been proposed [80, 81].

### 3.3. Magnitude of the VLE

Figure 8 displays vector length errors across four distinct zones, represented by different colors, and plotted against coordinate numbers on the x-axis. In Zone 1 (south), the error magnitude is minimal and consistent, with an average of 25.7 meters, a maximum of 27.2 meters, and a minimum of 24.2 meters. Zone 2 (mid-south) exhibited periodic fluctuations, with an average error of 32.9 meters, a maximum of 36.8 meters, and a minimum of 26.2 meters. Zones 3 (mid-north) and 4 (north) show a pronounced upward trend in error magnitude. Zone 3 has an average error of 48.6 meters, with a maximum of 52.5 meters and a minimum of 45.4 meters. Zone 4 displays the highest error values, with an average of 59.3 meters, a maximum of 61.2 meters, and a minimum of 58.1 meters. These increasing discrepancies are likely due to the positioning of the campus at the edge of UTM Zone 38, which can cause coordinate distortions. In general, while the southern zones maintain minimal length errors, the northern zones experience greater and greater discrepancies. This emphasizes the need for targeted corrections in these areas to enhance data accuracy. In GIS data, accuracy refers to how closely the data represent the true value of the measured entity, while precision indicates the exactness of the data description [82].

Errors can arise from various sources, such as outdated data, measurement inaccuracies, and improper data handling [83]. Precision without accuracy can lead to systematic errors, requiring adjustments to align data with real-world conditions [84]. In climate studies, such as those conducted in Ghana, discrepancies between different agro-ecological zones highlight the challenges in maintaining data accuracy across diverse geographical areas [85]. The analysis of GE imagery indicates that the most recent data from 2018 exhibit the highest accuracy, whereas the data from 2000 show the least accuracy [7]. This trend underscores a consistent improvement in the precision and dependability of satellite imagery, which underpins the data utilized by GE. Ensuring high data accuracy involves several quality assurance processes, such as validation checks, data cleansing, and regular audits, to maintain the integrity and reliability of the data throughout its lifecycle. Addressing these aspects helps minimize errors and improve the overall quality of the data used for decision-making and analysis [86].

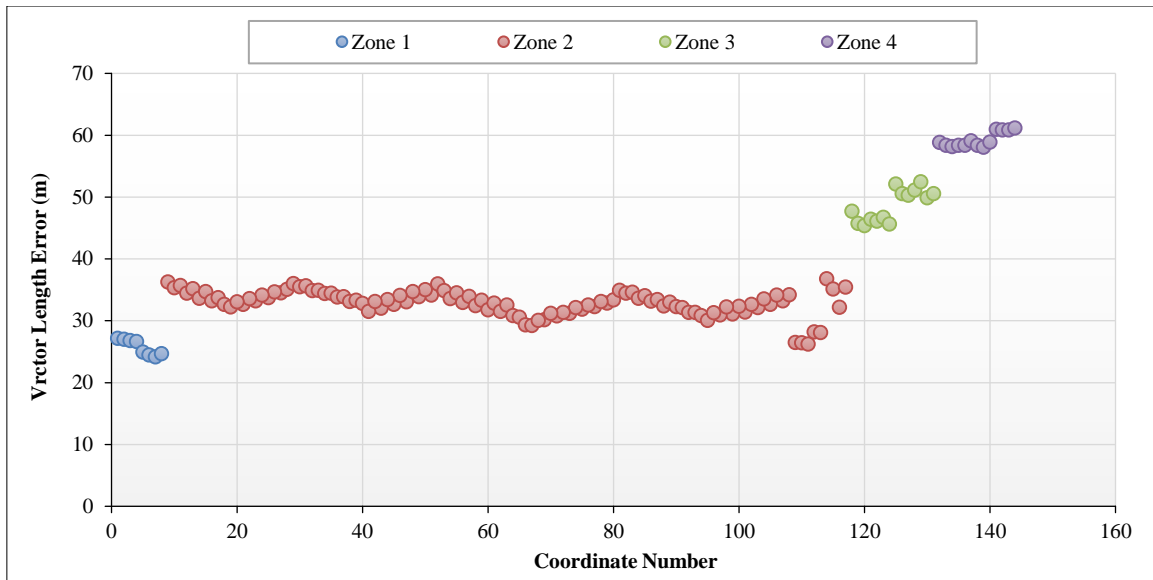


Figure 8. Vector length error magnitude by location

Figure 9 depicts a comparative analysis of spatial data derived from ABD, GE, and VLE, each distinguished by color coding in red, black, and blue, respectively. The figures, comprising mainly quadrilaterals and triangles, are annotated with numerical values, which likely indicate measurements pertinent to geometric assessments or discrepancies between the different data sources.

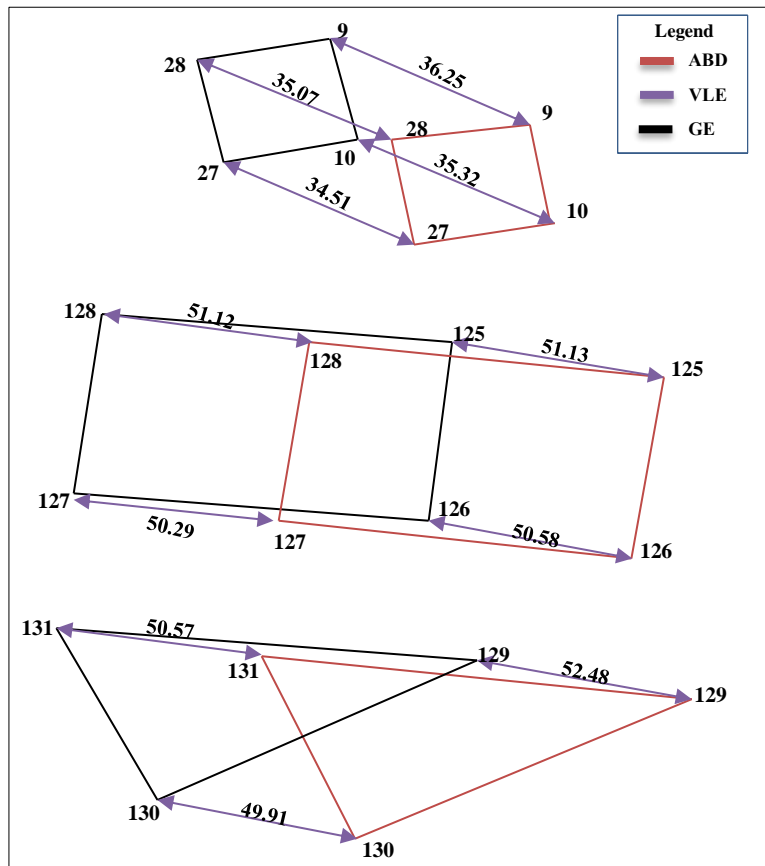


Figure 9. Example of coordinate shifting and VLE

In scientific and engineering contexts, ABDs are crucial for capturing the exact specifications of a constructed environment, while GEs provide geospatial data from a global perspective, which may be less precise due to satellite imaging limitations. The VLE possibly quantifies the deviations or inaccuracies between the ABD and the GE data, providing insights into the reliability and accuracy of remote sensing data compared to ground-truth architectural documents.

In brief, ABCs provide a reliable baseline for verifying spatial data, ensuring that construction aligns with design specifications [87]. VLEs, arising from instrument precision and human error, can distort spatial relationships, necessitating mitigation strategies [88]. GE offers accessible geospatial data, although its precision varies, making it useful for preliminary assessments but requiring careful consideration of its limitations [4]. Integrating GE with accurate ABCs and addressing VLEs enhances the reliability of geospatial analyses.

Figure 9 serves as a critical tool for visualizing and quantifying the spatial discrepancies that often arise in remote sensing applications, urban planning, and civil engineering. The numerical labels on each edge could represent the magnitude of vector discrepancies, which are essential for error analysis and correction in precision-dependent projects. By mapping these errors, researchers and practitioners can identify inconsistency patterns and apply corrective measures to enhance data reliability and application accuracy. Moreover, the structured presentation of these data through clear, color-coded distinctions facilitates an intuitive understanding of complex relationships and variations across the datasets, aiding in more accurate interpretations and decisions in project management and planning. Overall, this approach is indicative of a sophisticated analysis aimed at enhancing the accuracy and utility of spatial data in practical applications, reflecting a deep integration of theoretical knowledge and practical execution in GIS and construction management.

## 4. Conclusions

This study embarked on an incisive evaluation of geospatial accuracy within Google Earth (GE), a cornerstone tool for those requiring precise navigational and mapping capabilities. Our findings underscore the robust potential of GE in both academic and professional domains, confirming its reliability and precision. The research presented herein not only offers significant insights into the optimization of mapping practices but also underscores the strategic application of GE in future geospatial endeavors. This comparative analysis, which juxtaposes Google Earth's coordinates with actual on-ground measurements, serves as a pivotal step toward augmenting the tool's practical utility and securing its sustained prominence in the evolving digital mapping arena. The key findings of this study include the following:

- The adoption of the Wilcoxon signed-rank test, chosen for its versatility across varied data types and its robustness to non-normal distributions, proved to be an optimal fit for our methodological framework. This test highlighted statistically significant discrepancies between GE coordinates and actual surveyed data (ABD coordinates), notably with a Wilcoxon W-value of 0.0 and a p-value of  $2.23 \times 10^{-25}$  for East coordinates and a W-value of 359.0 with a p-value of approximately  $3.19 \times 10^{-22}$  for North coordinates.
- A regional analysis revealed varying degrees of coordinate displacement: southern zones exhibited minimal discrepancies, whereas northern zones showed significant divergence, particularly in the eastward measurements. This spatial variability underscores the necessity for region-specific adjustments to enhance the accuracy of GEs.
- This study further demonstrated the indispensable role of as-built drawings (ABDs) in capturing precise specifications of the built environment. Conversely, GE's global geospatial data, derived from satellite imaging, often lack the same level of precision, highlighting a critical area for improvement.

Furthermore, it is found that by synthesizing these insights, this research not only advances the precision and utility of spatial data in practical applications but also integrates theoretical knowledge with empirical analysis in the realms of GIS and construction management. This confluence sets a new benchmark for meticulousness and application in geospatial research, paving the way for future studies aimed at further refining the accuracy of digital mapping tools. It is also revealed that by elucidating the limitations in Google Maps' positioning accuracy, this study underscores potential usability issues and offers a foundation for future technological enhancements, thereby advancing the discourse in geospatial accuracy research.

Based on the key findings of this study, it is recommended that scholars investigate alternative mapping technologies and evaluate their accuracy across various regions of Saudi Arabia. Furthermore, an in-depth examination of the impact of environmental factors on the positioning accuracy of diverse mapping services could provide significant insights into optimizing geospatial data reliability.

## 5. Declarations

### 5.1. Data Availability Statement

The data presented in this study are available on request from the corresponding author.

### 5.2. Funding and Acknowledgements

The author extends his appreciation to Prince Sattam bin Abdulaziz University for funding this research work through the project number (PSAU/2023/01/25646).

### 5.3. Conflicts of Interest

The author declares no conflict of interest.

## 6. References

- [1] Bartłomiej, O., Jędrzej, M., & Janusz, Ć. (2017). Decoding of GPS data for single point positioning computation by using python programming language. *International Multidisciplinary Scientific GeoConference Surveying Geology and Mining Ecology Management, SGEM*, 17(22), 193–202. doi:10.5593/sgem2017/22/S09.024.
- [2] Prasai, R., Schwertner, T. W., Mainali, K., Mathewson, H., Kafley, H., Thapa, S., Adhikari, D., Medley, P., & Drake, J. (2021). Application of Google earth engine python API and NAIP imagery for land use and land cover classification: A case study in Florida, USA. *Ecological Informatics*, 66. doi:10.1016/j.ecoinf.2021.101474.
- [3] Anderson, K., Ryan, B., Sonntag, W., Kavvada, A., & Friedl, L. (2017). Earth observation in service of the 2030 Agenda for Sustainable Development. *Geo-Spatial Information Science*, 20(2), 77–96. doi:10.1080/10095020.2017.1333230.
- [4] Yu, L., & Gong, P. (2012). Google Earth as a virtual globe tool for Earth science applications at the global scale: progress and perspectives. *International Journal of Remote Sensing*, 33(12), 3966–3986. doi:10.1080/01431161.2011.636081.
- [5] Giuliani, G., Mazzetti, P., Santoro, M., Nativi, S., Bemmelen, J. Van, Colangeli, G., & Lehmann, A. (2020). Knowledge Generation Using Satellite Earth Observations to Support sustainable Development Goals (SDG): A Use Case on Land Degradation. *International Journal of Applied Earth Observation and Geoinformation*, 88. doi:10.1016/j.jag.2020.102068.
- [6] Zuliani, C., Santoro, V., Nugnes, M., & Colombo, C. (2021). Social Benefits Assessment of Earth Observation Missions Through the SDG2030. *International Astronautical Congress: IAC Proceedings*. 25-29 October, 2021, Dubai, United Arab Emirates.
- [7] Nwilo, P. C., Okolie, C. J., Onyegbula, J. C., Arungwa, I. D., Ayoade, O. Q., Daramola, O. E., Orji, M. J., Maduako, I. D., & Uyo, I. I. (2022). Positional accuracy assessment of historical Google Earth imagery in Lagos State, Nigeria. *Applied Geomatics*, 14(3), 545–568. doi:10.1007/s12518-022-00449-9.
- [8] Sheppard, S. R. J., & Cizek, P. (2009). The ethics of Google Earth: Crossing thresholds from spatial data to landscape visualisation. *Journal of Environmental Management*, 90(6), 2102–2117. doi:10.1016/j.jenvman.2007.09.012.
- [9] Clarke, P., Ailshire, J., Melendez, R., Bader, M., & Morenoff, J. (2010). Using Google Earth to conduct a neighborhood audit: Reliability of a virtual audit instrument. *Health & Place*, 16(6), 1224–1229. doi:10.1016/j.healthplace.2010.08.007.
- [10] Sharma, A., Wang, J., & Lennartson, E. M. (2017). Intercomparison of MODIS and VIIRS fire products in Khanty-Mansiysk Russia: Implications for characterizing gas flaring from space. *Atmosphere*, 8(6), 95. doi:10.3390/atmos8060095.
- [11] Du, H., Cai, W., Xu, Y., Wang, Z., Wang, Y., & Cai, Y. (2017). Quantifying the cool island effects of urban green spaces using remote sensing Data. *Urban Forestry & Urban Greening*, 27, 24–31. doi:10.1016/j.ufug.2017.06.008.
- [12] Kakooei, M., & Baleghi, Y. (2020). A two-level fusion for building irregularity detection in post-disaster VHR oblique images. *Earth Science Informatics*, 13(2), 459–477. doi:10.1007/s12145-020-00449-6.
- [13] Xiang, X., & Liu, Y. (2017). Understanding ‘change’ through spatial thinking using Google Earth in secondary geography. *Journal of Computer Assisted Learning*, 33(1), 65–78. doi:10.1111/jcal.12166.
- [14] Liang, J., Gong, J., & Li, W. (2018). Applications and impacts of Google Earth: A decadal review (2006–2016). *ISPRS Journal of Photogrammetry and Remote Sensing*, 146, 91–107. doi:10.1016/j.isprsjprs.2018.08.019.
- [15] Harris, L., Nel, R., Holness, S., Sink, K., & Schoeman, D. (2014). Setting conservation targets for sandy beach ecosystems. *Estuarine, Coastal and Shelf Science*, 150, 45–57. doi:10.1016/j.ecss.2013.05.016.
- [16] Strom, T. E. (2011). Space, Cyberspace and Interface: The Trouble with Google Maps. *M/C Journal*, 14(3), 370. doi:10.5204/mcj.370.
- [17] Jacobson, A., Dhanota, J., Godfrey, J., Jacobson, H., Rossman, Z., Stanish, A., Walker, H., & Riggio, J. (2015). A novel approach to mapping land conversion using Google Earth with an application to East Africa. *Environmental Modelling & Software*, 72, 1–9. doi:10.1016/j.envsoft.2015.06.011.
- [18] Ngom Vougat, R. R. B., Chouto, S., Aoudou Doua, S., Garabed, R., Zoli Pagnah, A., & Gonne, B. (2019). Using Google EarthTM and Geographical Information System data as method to delineate sample domains for an urban household surveys: The case of Maroua (Far North Region-Cameroon). *International Journal of Health Geographics*, 18(1), 1-12. doi:10.1186/s12942-019-0186-8.
- [19] Malarvizhi, K., Kumar, S. V., & Porchelvan, P. (2016). Use of High Resolution Google Earth Satellite Imagery in Landuse Map Preparation for Urban Related Applications. *Procedia Technology*, 24, 1835–1842. doi:10.1016/j.protcy.2016.05.231.
- [20] Langenkamp, J. P., & Rienow, A. (2023). Exploring the Use of Orthophotos in Google Earth Engine for Very High-Resolution Mapping of Impervious Surfaces: A Data Fusion Approach in Wuppertal, Germany. *Remote Sensing*, 15(7), 1818. doi:10.3390/rs15071818.
- [21] Fariz, T. R., Suhardono, S., Sultan, H., Rahmawati, D., & Arifah, E. Z. (2022). Land Cover Mapping in Lake Rawa Pening Using Landsat 9 Imagery and Google Earth Engine. *Journal of Environmental and Science Education*, 2(1), 1–6. doi:10.15294/jese.v2i1.55851.

- [22] Quijano, M. G., De La Cruz, A., Mielewczyk, M., & Cerra, D. (2007). Assessing refugee movement during the Israel - Lebanon crisis of 2006 using DMSP imagery. In American Society for Photogrammetry and Remote Sensing - 28<sup>th</sup> Canadian Symposium on Remote Sensing and ASPRS Fall Specialty Conference 2007, 28 October-1 November, Ottawa, Canada.
- [23] Hanberry, B. B. (2020). Classifying large wildfires in the United States by land cover. *Remote Sensing*, 12(18), 2966. doi:10.3390/RS12182966.
- [24] Inman, V. L., & Lyons, M. B. (2020). Automated inundation mapping over large areas using Landsat data and google earth engine. *Remote Sensing*, 12(8), 1348. doi:10.3390/RS12081348.
- [25] John, J., Chithra, N. R., & Thampi, S. G. (2019). Prediction of land use/cover change in the Bharathapuzha river basin, India using geospatial techniques. *Environmental Monitoring and Assessment*, 191(6), 354. doi:10.1007/s10661-019-7482-4.
- [26] Shekhar, S., Feiner, S., & Aref, W. G. (2015). From GPS and virtual globes to spatial computing - 2020. *GeoInformatica*, 19(4), 799–832. doi:10.1007/s10707-015-0235-9.
- [27] Brovelli, M. A., & Zamboni, G. (2012). Virtual globes for 4D environmental analysis. *Applied Geomatics*, 4(3), 163–172. doi:10.1007/s12518-012-0091-3.
- [28] Hung, K. C., Kalantari, M., & Rajabifard, A. (2016). Methods for assessing the credibility of volunteered geographic information in flood response: A case study in Brisbane, Australia. *Applied Geography*, 68, 37–47. doi:10.1016/j.apgeog.2016.01.005.
- [29] Kitalika, A., Machunda, R., Komakech, H., & Njau, K. (2018). Land-Use and Land Cover Changes on the Slopes of Mount Meru-Tanzania. *Current World Environment*, 13(3), 331–352. doi:10.12944/cwe.13.3.07.
- [30] Leroux, C., Jones, H., Pichon, L., Guillaume, S., Lamour, J., Taylor, J., Naud, O., Crestey, T., Lablee, J.-L., & Tisseyre, B. (2018). GeoFIS: An Open Source, Decision-Support Tool for Precision Agriculture Data. *Agriculture*, 8(6), 73. doi:10.3390/agriculture8060073.
- [31] Yazirlioğlu, L. (2021). Sustainable Design Considerations for Emotional Durability and Product Longevity Through Product Care Activities by Repair Enthusiasts. Master Thesis, Middle East Technical University, Ankara, Turkey.
- [32] Midekisa, A., Holl, F., Savory, D. J., Andrade-Pacheco, R., Gething, P. W., Bennett, A., & Sturrock, H. J. W. (2017). Mapping land cover change over continental Africa using Landsat and Google Earth Engine cloud computing. *PLoS ONE*, 12(9), 0184926. doi:10.1371/journal.pone.0184926.
- [33] Pulighe, G., Baiocchi, V., & Lupia, F. (2016). Horizontal accuracy assessment of very high-resolution Google Earth images in the city of Rome, Italy. *International Journal of Digital Earth*, 9(4), 342–362. doi:10.1080/17538947.2015.1031716.
- [34] Paredes-Hernández, C. U., Salinas-Castillo, W. E., Guevara-Cortina, F., & Martínez-Becerra, X. (2013). Horizontal positional accuracy of Google Earth's imagery over rural areas: a study case in Tamaulipas, Mexico. *Boletim de Ciências Geodésicas*, 19(4), 588–601. doi:10.1590/s1982-21702013000400005.
- [35] Wang, Y., Zou, Y., Henrickson, K., Wang, Y., Tang, J., & Park, B. J. (2017). Google Earth elevation data extraction and accuracy assessment for transportation applications. *PLoS ONE*, 12(4). doi:10.1371/journal.pone.0175756.
- [36] Rizeei, H. M., & Pradhan, B. (2019). Urban mapping accuracy enhancement in high-rise built-up areas deployed by 3d-orthorectification correction from worldview-3 and lidar imageries. *Remote Sensing*, 11(6), 692. doi:10.3390/rs11060692.
- [37] Pragada, A., & Rajan, K. S. (2023). Does Google Earth CRS induce bias with increasing UTM zone number? 2023 International Conference on Machine Intelligence for GeoAnalytics and Remote Sensing (MIGARS), Hyderabad, India. doi:10.1109/migars57353.2023.10064588.
- [38] Craglia, M., Goodchild, M. F., Annoni, A., Camara, G., Gould, M., Kuhn, W., Mark, D., Masser, I., Maguire, D., Liang, S., & Parsons, E. (2008). A position paper from the Vespucci Initiative for the Advancement of Geographic Information Science. *International Journal of Spatial Data Infrastructures Research*, 3, 146–167. doi:10.2902/1725-0463.2008.03.art9.
- [39] Salinas-Castillo, W. E., & Paredes-Hernández, C. U. (2014). Horizontal and vertical accuracy of Google Earth®: comment on “Positional accuracy of the Google Earth terrain model derived from stratigraphic unconformities in the Big Bend region, Texas, USA” by S.C. Benker, R.P. Langford and T.L. Pavlis. *Geocarto International*, 29(6), 625–627. doi:10.1080/10106049.2013.821176.
- [40] Vos, K., Splinter, K. D., Harley, M. D., Simmons, J. A., & Turner, I. L. (2019). CoastSat: A Google Earth Engine-enabled Python toolkit to extract shorelines from publicly available satellite imagery. *Environmental Modelling and Software*, 122. doi:10.1016/j.envsoft.2019.104528.
- [41] Bajaj, M., Sasaki, N., Tsusaka, T. W., Venkatappa, M., Abe, I., & Shrestha, R. P. (2024). Assessing changes in mangrove forest cover and carbon stocks in the Lower Mekong Region using Google Earth Engine. *Innovation and Green Development*, 3(3), 100140. doi:10.1016/j.igd.2024.100140.
- [42] Zurqani, H. A. (2024). High-resolution forest canopy cover estimation in ecodiverse landscape using machine learning and Google Earth Engine: Validity and reliability assessment. *Remote Sensing Applications: Society and Environment*, 33. doi:10.1016/j.rsase.2023.101095.

- [43] Ganjirad, M., & Bagheri, H. (2024). Google Earth Engine-based mapping of land use and land cover for weather forecast models using Landsat 8 imagery. *Ecological Informatics*, 80. doi:10.1016/j.ecoinf.2024.102498.
- [44] Habibie, M. I., Ramadhan, Nurda, N., Sencaki, D. B., Putra, P. K., Prayogi, H., Agustan, Sutrisno, D., & Bintoro, O. B. (2024). The development land utilization and cover of the Jambi district are examined and forecasted using Google Earth Engine and CNN1D. *Remote Sensing Applications: Society and Environment*, 34. doi:10.1016/j.rsase.2024.101175.
- [45] Merchant, M., Brisco, B., Mahdianpari, M., Bourgeau-Chavez, L., Murnaghan, K., DeVries, B., & Berg, A. (2023). Leveraging google earth engine cloud computing for large-scale arctic wetland mapping. *International Journal of Applied Earth Observation and Geoinformation*, 125. doi:10.1016/j.jag.2023.103589.
- [46] Gokool, S., Mahomed, M., Brewer, K., Naiken, V., Clulow, A., Sibanda, M., & Mabhaudhi, T. (2024). Crop mapping in smallholder farms using unmanned aerial vehicle imagery and geospatial cloud computing infrastructure. *Heliyon*, 10(5), e26913. doi:10.1016/j.heliyon.2024.e26913.
- [47] Luo, L., Wang, X., Guo, H., Lasaponara, R., Shi, P., Bachagha, N., Li, L., Yao, Y., Masini, N., Chen, F., Ji, W., Cao, H., Li, C., & Hu, N. (2018). Google earth as a powerful tool for archaeological and cultural heritage applications: A review. *Remote Sensing*, 10(10), 1558. doi:10.3390/rs10101558.
- [48] Ubukawa, T. (2013). An evaluation of the horizontal positional accuracy of Google and Bing satellite imagery and three roads data sets based on high resolution satellite imagery. Center for International Earth Science Information Network (CIESIN), The Earth Institute, Columbia University, New York, United States.
- [49] Lesiv, M., See, L., Bayas, J. C. L., Sturm, T., Schepaschenko, D., Karner, M., Moorthy, I., McCallum, I., & Fritz, S. (2018). Characterizing the spatial and temporal availability of very high resolution satellite imagery in Google Earth and Microsoft Bing Maps as a source of reference data. *Land*, 7(4), 118. doi:10.3390/land7040118.
- [50] Buka, I., Maruziva, R., & Nenhowe, P. (2015). A comparison of Google Earth extracted points with GPS surveyed points. *Ethiopian Journal of Environmental Studies and Management*, 8(5), 484. doi:10.4314/ejesm.v8i5.2.
- [51] Vanderhoof, M., Brunner, N., Beal, Y.-J., & Hawbaker, T. (2017). Evaluation of the U.S. Geological Survey Landsat Burned Area Essential Climate Variable across the Conterminous U.S. Using Commercial High-Resolution Imagery. *Remote Sensing*, 9(7), 743. doi:10.3390/rs9070743.
- [52] Goudarzi, M. A., & Landry, R. J. (2017). Assessing horizontal positional accuracy of Google Earth imagery in the city of Montreal, Canada. *Geodesy and Cartography*, 43(2), 56–65. doi:10.3846/20296991.2017.1330767.
- [53] Bärghman, J., Smith, K., & Werneke, J. (2015). Quantifying drivers' comfort-zone and dread-zone boundaries in left turn across path/opposite direction (LTAP/OD) scenarios. *Transportation Research Part F: Traffic Psychology and Behaviour*, 35, 170–184. doi:10.1016/j.trf.2015.10.003.
- [54] Elwood, S., Goodchild, M. F., & Sui, D. Z. (2012). Researching Volunteered Geographic Information: Spatial Data, Geographic Research, and New Social Practice. *Annals of the Association of American Geographers*, 102(3), 571–590. doi:10.1080/00045608.2011.595657.
- [55] Frey, B. B. (2023). Wilcoxon Signed Ranks Test. In *There's a Stat for That! What to Do & When to Do It*. Sage Publications, Thousand Oaks, United States doi:10.4135/9781071909775.n17.
- [56] Li, S., Dragicevic, S., Castro, F. A., Sester, M., Winter, S., Coltekin, A., Pettit, C., Jiang, B., Haworth, J., Stein, A., & Cheng, T. (2016). Geospatial big data handling theory and methods: A review and research challenges. *ISPRS Journal of Photogrammetry and Remote Sensing*, 115, 119–133. doi:10.1016/j.isprsjprs.2015.10.012.
- [57] Silva, D. S., & Holanda, M. (2022). Applications of geospatial big data in the Internet of Things. *Transactions in GIS*, 26(1), 41-71. doi:10.1111/tgis.12846.
- [58] Escamilla Molgora, J. M., Sedda, L., & Atkinson, P. M. (2020). Biospytial: Spatial graph-based computing for ecological Big Data. *GigaScience*, 9(5), 1-25. doi:10.1093/gigascience/giaa039.
- [59] Goodchild, M. F., & Li, L. (2012). Assuring the quality of volunteered geographic information. *Spatial Statistics*, 1, 110–120. doi:10.1016/j.spasta.2012.03.002.
- [60] Li, D., Zhang, J., & Wu, H. (2012). Spatial data quality and beyond. *International Journal of Geographical Information Science*, 26(12), 2277–2290. doi:10.1080/13658816.2012.719625.
- [61] West Meiers, M. (2022). The Independent Evaluation Group (IEG) of the World Bank Group: Influences on Evaluation Structures and Practices Globally and in the Americas. *The Institutionalisation of Evaluation in the Americas*. Palgrave Macmillan, Cham, Switzerland. doi:10.1007/978-3-030-81139-6\_15.
- [62] Li, W., & Hsu, C. Y. (2022). GeoAI for Large-Scale Image Analysis and Machine Vision: Recent Progress of Artificial Intelligence in Geography. *ISPRS International Journal of Geo-Information*, 11(7), 385. doi:10.3390/ijgi11070385.

- [63] Fisher, P. F., & Tate, N. J. (2006). Causes and consequences of error in digital elevation models. *Progress in Physical Geography*, 30(4), 467–489. doi:10.1191/0309133306pp492ra.
- [64] Li, J., Lewis, J., Rowland, J., Tappan, G., & Tieszen, L. L. (2004). Evaluation of land performance in Senegal using multi-temporal NDVI and rainfall series. *Journal of Arid Environments*, 59(3), 463–480. doi:10.1016/j.jaridenv.2004.03.019.
- [65] Duckham, M. (2013). *Decentralized Spatial Computing*. Springer, Berlin, Germany. doi:10.1007/978-3-642-30853-6.
- [66] EPSG:32638 (2024). WGS 84/ UTM zone 38N. Spatial Reference. Available online: <https://spatialreference.org/ref/epsg/32638/> (accessed on July 2024).
- [67] Holoway, G., Lacombe, D., & LeSage, J. P. (2007). Spatial econometric issues for bio-economic and land-use modelling. *Journal of Agricultural Economics*, 58(3), 549–588. doi:10.1111/j.1477-9552.2007.00127.x.
- [68] Endricks, N. P. H., Smith, A., & Sumner, D. A. (2014). Crop supply dynamics and the illusion of partial adjustment. *American Journal of Agricultural Economics*, 96(5), 1469–1491. doi:10.1093/ajae/aau024.
- [69] Sohl, T. L., Sayler, K. L., Drummond, M. A., & Loveland, T. R. (2007). The fore-sce model: A practical approach for projecting land cover change using scenario-based modeling. *Journal of Land Use Science*, 2(2), 103–126. doi:10.1080/17474230701218202.
- [70] Hinton, J. W., Hurst, J. E., Kramer, D. W., Stickles, J. H., & Frair, J. L. (2022). A model-based estimate of winter distribution and abundance of white-tailed deer in the Adirondack Park. *PLOS ONE*, 17(8), e0273707. doi:10.1371/journal.pone.0273707.
- [71] Nelson, G. C., & Hellerstein, D. (1997). Do Roads Cause Deforestation? Using Satellite Images in Econometric Analysis of Land Use. *American Journal of Agricultural Economics*, 79(1), 80–88. doi:10.2307/1243944.
- [72] Lawler, J. J., Lewis, D. J., Nelson, E., Plantinga, A. J., Polasky, S., Withey, J. C., Helmers, D. P., Martinuzzi, S., Penningtonh, D., & Radeloff, V. C. (2014). Projected land-use change impacts on ecosystem services in the United States. *Proceedings of the National Academy of Sciences of the United States of America*, 111(20), 7492–7497. doi:10.1073/pnas.1405557111.
- [73] Lark, T. J., Mueller, R. M., Johnson, D. M., & Gibbs, H. K. (2017). Measuring land-use and land-cover change using the U.S. department of agriculture’s cropland data layer: Cautions and recommendations. *International Journal of Applied Earth Observation and Geoinformation*, 62, 224–235. doi:10.1016/j.jag.2017.06.007.
- [74] Fritz, S., See, L., & Rembold, F. (2010). Comparison of global and regional land cover maps with statistical information for the agricultural domain in Africa. *International Journal of Remote Sensing*, 31(9), 2237–2256. doi:10.1080/01431160902946598.
- [75] Xu, Y., Yu, L., Feng, D., Peng, D., Li, C., Huang, X., Lu, H., & Gong, P. (2019). Comparisons of three recent moderate resolution African land cover datasets: CGLS-LC100, ESA-S2-LC20, and FROM-GLC-Africa30. *International Journal of Remote Sensing*, 40(16), 6185–6202. doi:10.1080/01431161.2019.1587207.
- [76] Vancutsem, C., Marinho, E., Kayitakire, F., See, L., & Fritz, S. (2013). Harmonizing and combining existing land cover/land use datasets for cropland area monitoring at the African continental scale. *Remote Sensing*, 5(1), 19–41. doi:10.3390/rs5010019.
- [77] Hua-Mei Chen, Varshney, P. K., & Arora, M. K. (2003). Performance of mutual information similarity measure for registration of multitemporal remote sensing images. *IEEE Transactions on Geoscience and Remote Sensing*, 41(11), 2445–2454. doi:10.1109/tgrs.2003.817664.
- [78] Townshend, J. R. G., Gurney, C., McManus, J., & Justice, C. O. (1992). The Impact of Misregistration on Change Detection. *IEEE Transactions on Geoscience and Remote Sensing*, 30(5), 1054–1060. doi:10.1109/36.175340.
- [79] Carmel, Y., Dean, D. J., & Flather, C. H. (2001). Combining location and classification error sources for estimating multi-temporal database accuracy. *Photogrammetric Engineering and Remote Sensing*, 67(7), 865–872.
- [80] Carmel, Y. (2004). Controlling data uncertainty via aggregation in remotely sensed data. *IEEE Geoscience and Remote Sensing Letters*, 1(2), 39–41. doi:10.1109/LGRS.2004.823453.
- [81] Zhang, M., Lin, H., Zeng, S., Li, J., Shi, J., & Wang, G. (2013). Impacts of plot location errors on accuracy of mapping and scaling up aboveground forest carbon using sample plot and Landsat tm data. *IEEE Geoscience and Remote Sensing Letters*, 10(6), 1483–1487. doi:10.1109/LGRS.2013.2260719.
- [82] Jitkajornwanich, K., Vateekul, P., Panboonyuen, T., Lawawirojwong, S., & Srisophon, S. (2017). Road map extraction from satellite imagery using connected component analysis and landscape metrics. 2017 IEEE International Conference on Big Data (Big Data), Boston, United States. doi:10.1109/bigdata.2017.8258330.
- [83] Rogan, J., & Miller, J. (2006). Integrating GIS and Remotely Sensed Data for Mapping Forest Disturbance and Change. *Understanding Forest Disturbance and Spatial Pattern*, 133–171. doi:10.1201/9781420005189.ch6.
- [84] Pascual, M. S. (2022). GIS Data: A Look at Accuracy, Precision, and Types of Errors, GIS Lounge. Geographyrealm, Santa Clara, United States. Available online: <https://www.gislounge.com/gis-data-a-look-at-accuracy-precision-and-types-of-errors/> (accessed on July 2024).

- [85] Wetterhall, F., Winsemius, H. C., Dutra, E., Werner, M., & Pappenberger, E. (2015). Seasonal predictions of agro-meteorological drought indicators for the Limpopo basin. *Hydrology and Earth System Sciences*, 19(6), 2577–2586. doi:10.5194/hess-19-2577-2015.
- [86] Atlan. (2023). *Data Accuracy in 2024: A Roadmap for Data Quality*. Atlan Pte. Ltd, Singapore. Available online: <https://atlan.com/data-accuracy-101-guide/> (accessed on May 2024).
- [87] Sattineni, A., & Bradford, R. H. (2011). Estimating with BIM: A survey of US construction companies. *Proceedings of the 28th International Symposium on Automation and Robotics in Construction, ISARC 2011*, 564–569. doi:10.22260/isarc2011/0103.
- [88] Li, Z., Zhu, C., & Gold, C. (2004). *Digital Terrain Modeling*. CRC Press, Boc Raton, United States. doi:10.1201/9780203357132.